Saturation-matric potential relations in gravel

Tetsu K. Tokunaga, Jiamin Wan, and Keith R. Olson

Earth Sciences Division, Lawrence Berkeley National Laboratory, Berkeley, California, USA

[1] Some environmentally sensitive unsaturated zone sediments, such as those underlying radioactive waste tanks in Hanford (Washington State), contain large fractions of gravels and coarse sands. Coarse, granular media are also included in designs of engineered capillary barriers for subsurface waste isolation. Thus knowledge of the unsaturated hydraulic properties of gravels is needed to understand flow and transport in these critical settings. When standard methods for measuring moisture characteristics or water retention relations are used for gravels, corrections are needed in the near-zero region of matric (pressure) potentials. The need for correction results from gravity stratification of saturation profiles within even short sample columns. Such a correction method was developed and used to determine drainage curves for Hanford gravels having characteristic grain sizes of 8.0–9.5, 4.8–5.3, and 2.0–2.4 mm. In 30 mm tall sample columns, gravity corrections were essential for the 9 and 5 mm gravels and less significant for the 2 mm gravel. Validity of the correction method was demonstrated through accurately reconstructing average column saturation-potential relations from their predicted local saturation-potential relations. The method and results presented here are part of an ongoing study on Hanford gravels and on limits to classical unsaturated hydraulic scaling encountered at large grain sizes.   *INDEX TERMS:* 1866 Hydrology: Soil moisture; 1875 Hydrology: Unsaturated zone; *KEYWORDS:* capillary, gravel, gravity, matric, saturation, unsaturated

1. Introduction

[2] Gravels and coarse sands make up significant portions of some environmentally important sediments. For example, the Hanford formation vadose zone underlying radioactive waste tanks in south central Washington State contains substantial regions characterized as coarse sands, gravelly sands, and sandy gravels [*Rhoades et al.*, 1992]. Well-sorted, coarse-textured media are also main components in capillary barrier designs for minimizing seepage through wastes buried in the subsurface [*Conca et al.*, 1998]. Knowledge of moisture characteristics or water retention relations is needed to predict hydrostatic conditions, as well as flow and transport in these coarse unsaturated porous media. Although a number of methods are available for determining moisture characteristic relations [*Klute*, 1986], measurements on coarse sands and gravels in the intermediate saturation (S) range present challenges because significant changes in saturation occur over matric head (h) intervals that are shorter than typical column heights. The matric head at the top of a column of length L is exactly $h_b - L$ under hydrostatic conditions, where h_b is the matric head at the bottom of the column. At matric potentials close to zero, the upper portion of an equilibrium gravel column can be significantly less in saturation than the bottom portion. Thus, for measuring S(h) relations of very coarse-textured sediments, keeping the column height short is not

only desirable for minimizing approximately L^2-dependent equilibration times [*Klute*, 1986], but also for minimizing equilibrium S gradients. Since the column height needs to remain tall enough to include multiple gravel grain diameters, it cannot be made short enough to yield insignificant saturation differences along the vertical axis. Errors in associating average column S values to the desired S(h) relation may be diminished by referencing the regulated h to the column's half-height elevation, but will not be completely eliminated [*Liu and Dane*, 1995]. This problem is illustrated in an example shown in Figure 1. An example exact S(h) drainage characteristic is shown as the solid curve. The whole column average S(h) relation for a 30 mm tall system was then obtained as a moving average with 30 mm S(h) averaging, centered about the average h (i.e., the h associated with the horizontal mid-plane). Errors associated with averaged S values are especially large in the vicinity of highest water capacity (highest dS/dh), and become insignificant at low saturation. At h = 0 mm, the average S value is 22% less than the true S(0 mm) in this example. At h = −10 mm, the average S is 11% higher than the true S(−10 mm). Since such errors are significant in themselves, and since they impart much larger errors for estimates of unsaturated hydraulic conductivities, corrections for gravity-stratified saturation profiles are important.

[3] Several methods to obtain correct saturation-potential relations under these conditions have been presented in recent years. Measurements of hydrostatic saturation profiles for water and TCE, obtained by dual-energy gamma attenuation, were used to directly determine local capillary
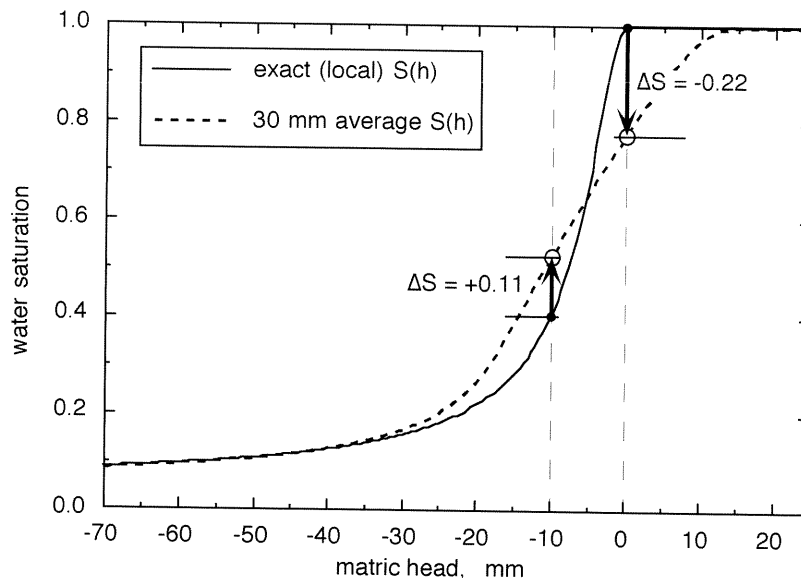
Figure 1. Comparison between an exact drainage curve for a gravel and the average saturation versus average matric head relation for a 30 mm tall column. The reference elevation for the average matric head is located at the horizontal midplane of the column. Example averaging errors at matric head values of 0 and −10 mm are shown.

pressure relations by *Dane et al.* [1992]. Similar tall-column profiling approaches have been used in much earlier studies [*Buckingham*, 1907; *Leverett*, 1941; *Luthin and Day*, 1955], albeit with less sophisticated technology. *Liu and Dane* [1995] developed a computational method that accounts for density and gravity effects in fitting functional relations such as that of *Brooks and Corey* [1964] to immiscible fluids. *Schroth et al.* [1996] developed a method based on fitting the *van Genuchten* [1980] expression for the h-dependent volumetric water content to numerically subdivided sample layers. More recently, *Jalbert and Dane* [2001] developed a very general correction procedure that does not assume a particular functional form of the saturation-potential relation. In this paper, we present an alternative approach to accounting for hydrostatic saturation variations within vertical sample columns in the determination of moisture characteristics. Our experiment-based approach develops from the analogy between equilibrating samples on a suction plate device and virtual translations of a reference sediment volume relative to a free water surface. The resulting correction formulas are special cases of solutions given by *Jalbert and Dane* [2001] who presented a different analysis. Our method was applied to data from 3 gravel columns, to obtain gravity-corrected S(h) relations. To our knowledge, these are the first reported gravity-corrected drainage moisture characteristics for gravels. The calculated S(h) relations were tested through comparisons of their predicted hydrostatic column-integrated average values against their measured average saturations.

2. Correction Method

[4] Our analysis begins with assuming that a homogeneous sample of porous medium on a suction plate [*Haines*, 1930] device is equivalent to a segment within an arbitrarily tall column of the same material in equilibrium with a water table. For the case of desaturating a sample, the reference tall column has also equilibrated by drainage from an initially saturated state. Conversely, for the case of a saturating sample, the tall reference column has equilibrated via capillary rise from an initially dry state. The drainage process within a sample on a suction plate is then analogous to virtual displacements of a segment of porous medium up the vertical (drained) column. Likewise, the wetting process within a sample is analogous to virtually descending down the vertical (imbibition) column. In general, the volume of water in the column at any particular equilibrium condition, i, is

$$V_w(i) = A \int_{h_b(i)-L}^{h_b(i)} \theta_w dh \qquad (1)$$

when the matric(pressure) head at the bottom surface is $h_b(i)$, A is the column cross-sectional area, and θ_w is the volumetric water content.

[5] The correction procedure will be developed here for initial drainage curves that start with the porous medium fully saturated [*Klute*, 1986], although it should be noted that the same procedure is applicable to main drainage (starting with entrapped air) and main wetting curves. A specific example of progressive desaturation is shown in Figure 2. We start with an initially fully saturated, 30 mm tall gravel column, with its horizontal mid-plane at h = 0 mm (Figure 2a). In this example, the pores at the top surface remain water saturated at h_L = −15 mm. Since only equilibrium conditions are considered, h_L will be referred to as h_b − L in the following analysis. The matric head at the bottom of the column is next lowered by Δh. In this illustration, Δh = −5 mm (going from h_b = +15 mm to h_b = +10 mm), equivalent to a 5 mm upwards virtual translation of the sample relative to the water table. The new equilibrium state is represented by the area outlined by the thick shaded line in Figure 2b, and the volumetric outflow,
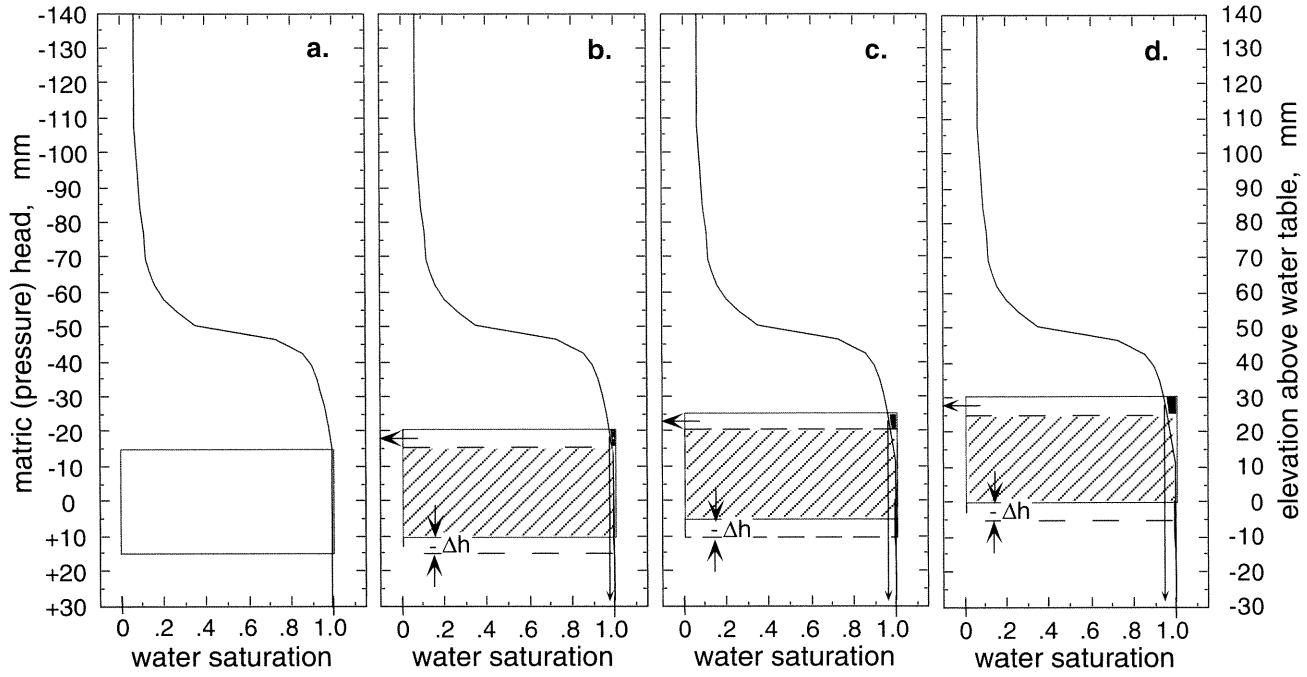
Figure 2. Illustration of the correction procedure associated with samples at higher saturations and equations (3a) and (3b). The step changes in matric head shown here are −5 mm. The hatched areas represent segments of S(h) that both the initial and final state have in common and are thus not associated with outflow. The black areas represent the differences between volume integrals for water contained in the sample at two adjacent equilibration steps and thus are associated with volumetric outflow.

$\Delta V_w(i,j)$, accompanying this change is represented by the black area within the $-20 < h < -15$ mm range. The indices i and j refer respectively to initial and final states of a single step change in h. Thus the volumetric outflow resulting from this Δh of -5 mm can only be associated with the uppermost 5 mm of the 30 mm gravel column. From equation (1),

$$\Delta V_w(i,j) = A \int_{h_b(i)-L}^{h_b(i)} \theta_w dh - A \int_{h_b(j)-L}^{h_b(j)} \theta_w dh \qquad (2a)$$

$$\Delta V_w(i,j) = nA \int_{h_b(i)-L}^{h_b(i)} S dh - nA \int_{h_b(j)-L}^{h_b(j)} S dh \qquad (2b)$$

where n is the total porosity and S is the water saturation. This subtraction eliminates the common regions of the integrals contained within both initial and final states, i.e., the hatched area within Figure 2b, such that

$$\frac{\Delta V_w(i,j)}{nA} = \int_{h_b(j)}^{h_b(i)} S dh - \int_{h_b(j)-L}^{h_b(i)-L} S dh \qquad (2c)$$

The first and second integrals on the RHS are associated with the saturations at the lower and upper 5 mm regions that bound the common regions. Thus

$$\bar{S}(h_b(i,j) - L) = \bar{S}(h_b(i,j)) + \frac{1}{nA}\frac{\Delta V_w(i,j)}{\Delta h} \qquad (3a)$$

where $\Delta h = -5$ mm, $S(h_b(i,j)-L)$ is the average saturation within the upper 5 mm column section after equilibration at the jth step, and $S(h_b(i,j))$ is the volume-averaged saturation within the lower 5 mm column section. The correction method is considered satisfactory when differences between calculated $S(h_b(i,j)-L)$ and exact S(h) relations are of experimentally indistinguishable magnitudes. This will be demonstrated later through reconstruction of measured column-averaged S(h) from integration of calculated $S(h_b(i,j)-L)$. Note that this procedure more generally amounts to determining the saturation within the upper column section (of thickness $|\Delta h|$), based on knowledge of the saturation within the bottom column section. When the nonwetting fluid density is negligible, and when only the first term in the summation is nonvanishing, the more general equation (21) of *Jalbert and Dane* [2001] is equivalent to equation (3a) above. The higher terms in the *Jalbert and Dane* [2001] summation vanish for the process described here because they represent the negligible moisture capacity of a rigid porous medium at positive pressure potentials. Since the h = 0 plane is still above the bottom column section, the latter saturation is unity, and

$$\bar{S}(h_b(i,j) - L) = 1 - \frac{1}{nA}\frac{\Delta V_w(i,j)}{\Delta h} \qquad (3b)$$

The bottom of the column is equilibrated to progressively lower potentials, and associated volumetric outflows are used to determine lower values of $S(h_b(i,j)-L)$ using equation (3b). Three successive drainage equilibrations are shown in Figures 2b–2d, with their associated $h_b(i,j)-L$
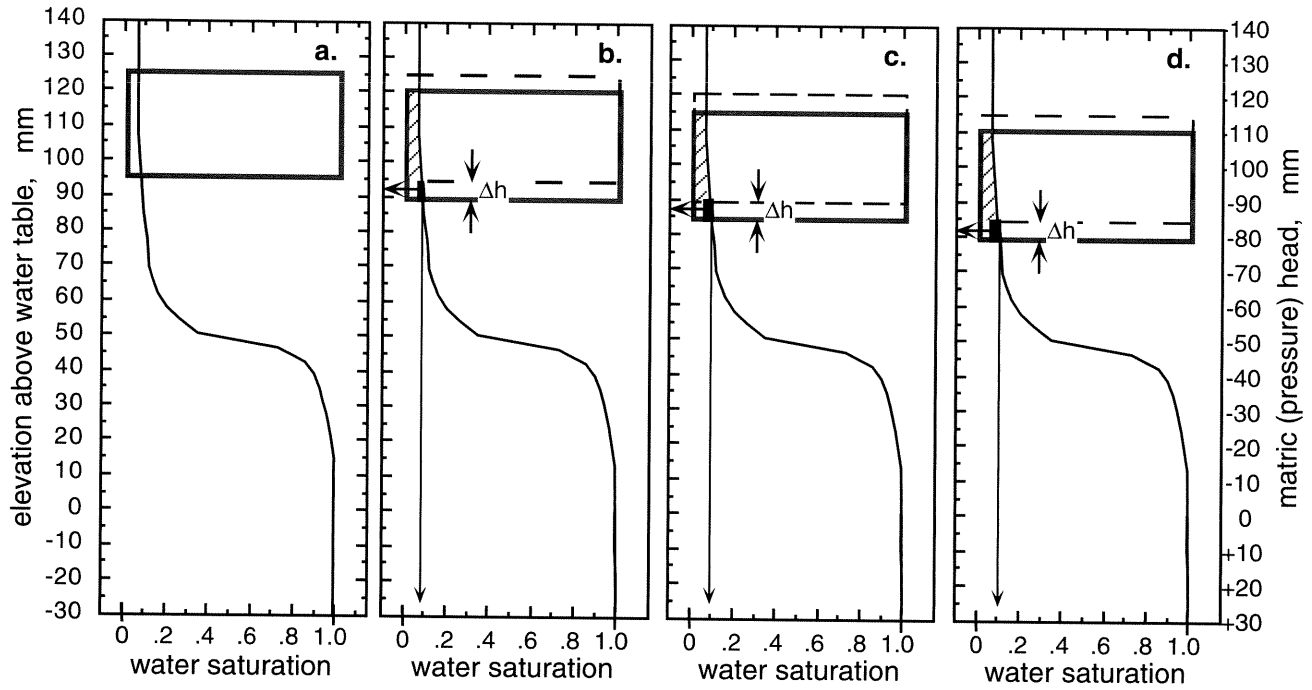
Figure 3. Illustration of the correction procedure associated with samples at lower saturations and equation 4. The step changes in matric head shown here are +5 mm. The hatched areas represent segments of S(h) that both the initial and final state have in common and are thus not associated with inflow. The black areas now are associated with volumetric inflow.

and $S(h_b(i,j)-L)$ values indicated by arrows. When $h_b(i,j)$ takes on values negative enough to cause desaturation at the bottom section of the sample, equation (3a) must be used instead of equation (3b) since $S(h_b(i,j))$ is no longer unity. The $S(h_b(i,j))$ used in subsequent calculations are obtained from previous calculated $S(h_b(i,j)-L)$ values. As an example, $S(-27.5$ mm) calculated by equation (3b) and illustrated in Figure 2d, can be used later to calculate $S(-57.5$ mm). Since such dependence on previously calculated $S(h_b(i,j)-L)$ values imparts higher uncertainties for estimating lower values of saturation, a slightly different correction approach for this region will be presented next.

[6] After completing a sequence of drainage equilibration steps to a point where decreases in matric head of magnitude Δh impart negligible drainage, gravity corrections can be applied in a slightly different manner in the lower saturation region of the moisture characteristic. In this region, greater local saturation changes occur within the lower section of the soil rather than in the upper section. Thus the upper section can be assigned a "residual" saturation value obtained from column-averaged S at low h. We then apply the above calculations in reverse, moving in positive Δh increments back toward higher S in order to determine the saturation within the bottom 5 mm segment of the sample. This procedure is illustrated in Figure 3, with the calculated saturation in the bottom 5 mm segment obtained from

$$\bar{S}(h_b(i,j)) = \bar{S}(h_b(i,j)-L) + \frac{1}{nA}\frac{\Delta V_w(i,j)}{\Delta h} \qquad (4)$$

Thus, in this case the saturation within the bottom section (Δh in thickness) is determined based on known, negligibly

changing S within the overlying region. This result is a special case of equation (24) of *Jalbert and Dane* [2001], for reasons similar to those discussed previously, with the only difference being that here we reference insignificant capacitance of the residual saturation region rather than the fully saturated region of the water retention curve. Since these equation (4) calculations build on "residual" saturation values, $S(h_b(i,j)-L)$, that only vary slightly with h, they are more reliable than equation (3a) when applied to the lower saturation range. In other words, the preferred equation to use is the one that utilizes a previously calculated S of lower absolute uncertainty. Typically, the previously calculated S that has the smallest $\Delta S/\Delta h$ will meet this condition. Thus the best approach typically combines equations (3a), (3b), and (4) for the high and low saturation ranges, respectively.

3. Experimental Materials and Methods

[7] The gravel samples were obtained from the Hanford Site in south central Washington State. These Hanford formation gravels and sandy gravels were deposited during cataclysmic floods released from Pleistocene ice-dammed lakes. Samples were excavated from Site 218-E-12B, in the north-east corner of the 200-East Area [*Rhoades et al.*, 1992]. Gravels were sieved into 8.0–9.5, 4.8–5.3, and 2.0–2.4 mm size fractions for testing of approximately monodisperse media. These three samples will be referred to as 9, 5, and 2 mm gravels, respectively. The overall shapes of the gravels were similar, having sphericities of about 0.7 and roundness of about 0.6 [*Krumbein and Sloss*, 1963].

[8] The gravels were prewetted by immersion in water, at subatmospheric pressure (2.3 kPa, absolute) overnight to
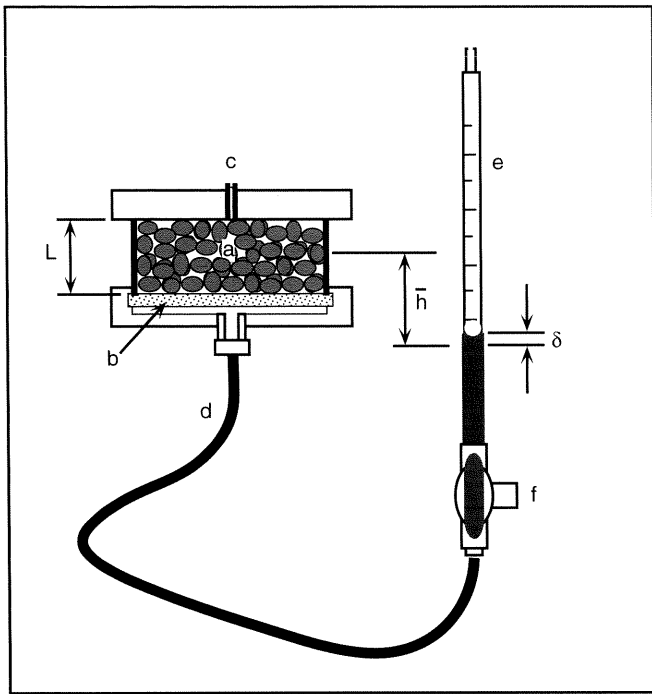
Figure 4. Haines apparatus for measuring average saturation versus average matric head. Components are a, porous medium; b, fritted glass plate; c, vent to atmospheric pressure; d, outflow tube; e, 10 mL pipette reservoir; and f, port for draining and filling the system. Other parameters shown are L, the column height; h, the average matric head; and δ, capillary rise in the pipette reservoir.

bring the intragranular pores to effective saturation. Gravels were then packed into water-filled, modified large Tempe cells (Soilmoisture Equipment Corp., Goleta, CA) with 82.6 mm ID, 30 mm tall sample chambers. This packing yielded initially saturated columns. The bottom end cap supported a fritted glass plate (Por C plates, Ace Glass, Vineland, NJ), which was connected to an outflow pipette (Figure 4). The Por C plates have an air-entry h ≈ −440 mm, and a saturated hydraulic conductivity of about 2×10^{-5} m s^{-1}. The 7.9 mm ID plastic outflow pipette had a capillary rise, δ, of 1 ±1 mm. The capillary rise-corrected water level in the outflow pipette was adjusted to 1 mm below the upper surface of the gravel pack at the start of an experiment. The pipette was then lowered such that the corrected meniscus elevation was maintained at 5 mm below the upper gravel surface. If drainage occurs, the pipette must be periodically shifted downward to maintain the meniscus elevation at the targeted level. Upon reaching a new equilibrium drainage condition, the volumetric outflow for this increment $(\Delta V_w(i,j))$ is recorded. The pipette is then lowered and the corrected meniscus elevation maintained at 10 mm below the upper gravel surface until the next equilibrium $\Delta V_w(i,j)$ is obtained. This procedure is repeated in 5 mm steps until a "residual" saturation condition was approached, where further decreases in the reservoir elevation yielded $\Delta V_w(i,j)$ less than 0.05 mL per 5 mm Δh. Collection of a series of $\Delta V_w(i,j)/\Delta h$ data, along with determination of the porosity of the gravel pack permitted calculation of gravity-corrected S(h) relations using equations (3) and (4), as well as uncorrected S(h) relations.

4. Results and Discussion

[9] Column-averaged S(h) and gravity-corrected S(h) data for the 9 mm gravel are presented in Figure 5. For this coarse gravel, gravity corrections to S(h) are clearly needed. The uncorrected and gravity corrected data follow distinctly different trends in the near-zero matric head region. Three additional curves based on the gravity-corrected S(h) results are also included. The first of these curves is fit to the gravity-correct S(h), using van Genuchten's [1980] method with $\alpha^{-1} = 4.5$ mm, n = 2.13, and a residual saturation of 0.044. The van Genuchten parameter m = 1 − (1/n) in all applications presented here. Most of the
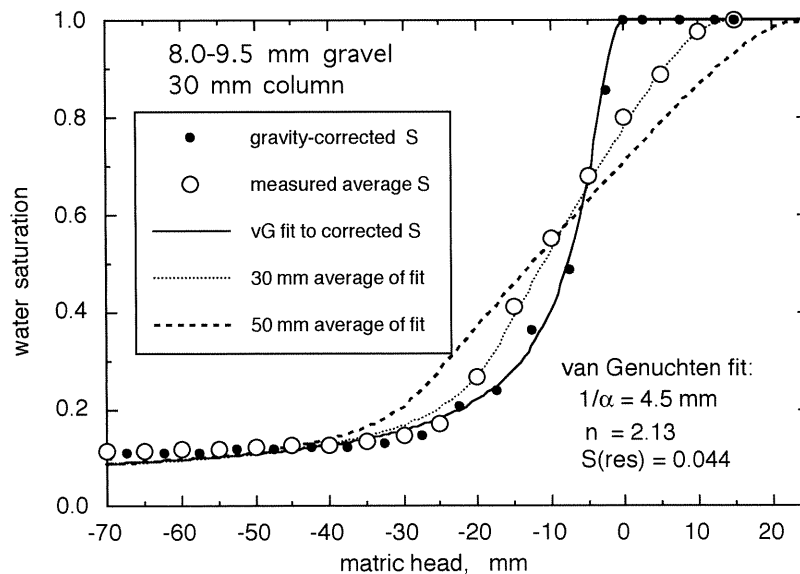

Figure 5. Drainage moisture characteristic for the 9 mm gravel.
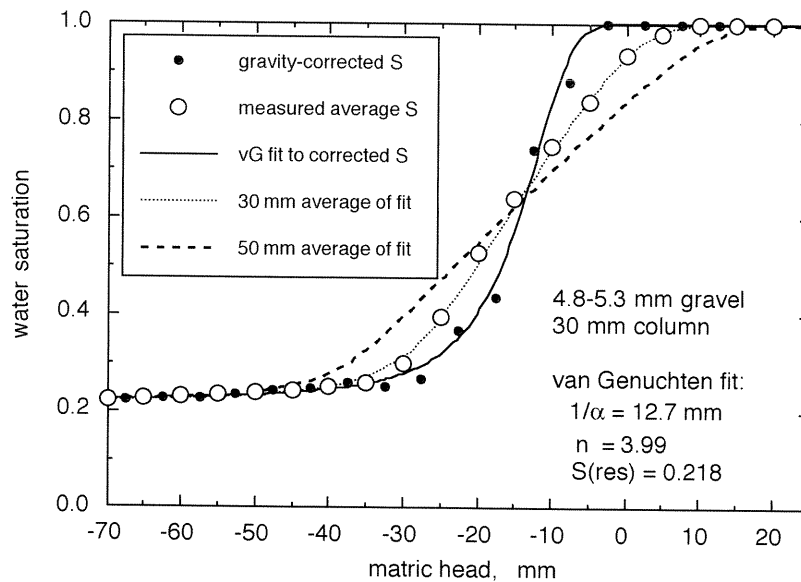
Figure 6. Drainage moisture characteristic for the 5 mm gravel.

residual saturation in all of these gravels is associated with their intragranular porosity. It should be noted that van Genuchten relations are only used to fit gravity-corrected results. *Brooks and Corey* [1964] relations were not used because air-entry values of gravels are very close to (within 5 mm Δh) or essentially equal to zero, and because some S(h) relations in gravels appear to exhibit continuity in $\Delta S/\Delta h$ within this region and at h = 0. The correction depends only on experimentally obtained measurements, and not on any specific model of S(h). The other two curves in Figure 5 were obtained as running averages of the fit S(h) over 30 and 50 mm matric head intervals, in the manner previously described for Figure 1. In fact, the van Genuchten fit and 30 mm average curve are identical to the curves presented in the earlier example. Since the column height is 30 mm, the 30 mm moving average should closely match the uncorrected S(h) data. The agreement between the calculated

30 mm moving average S(h) and the original column-average S(h) indicates that the gravity correction procedure is satisfactory. The 50 mm moving average shown in Figure 5 was calculated only to show predicted uncorrected results with larger departures from the local S(h) for a hypothetical experiment done on a taller column.

[10] The data and fits for the 5 mm gravel are shown in Figure 6. Again, necessity of gravity corrections is demonstrated through distinctly different trends in the near-zero matric head region for the column-averaged and local S(h). As before, the 3 curves represent the van Genuchten fit to the gravity-corrected data, a 30 mm moving average S(h), and a 50 mm moving average S(h), with the latter curves based on the van Genuchten fit. The parameters for this fit are given in Figure 6. As before, the fact that the 30 mm moving average S(h) curve fits the uncorrected S(h) data provides support for the methodology. Again, the 50 mm
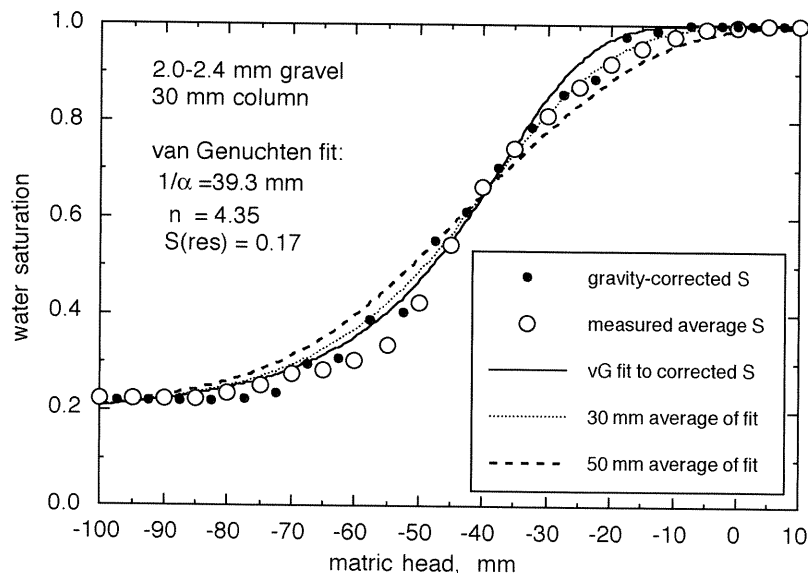

Figure 7. Drainage moisture characteristic for the 2 mm gravel.

moving average is included only to illustrate magnification of errors when averaging over a longer column length.

[11] Results from the 2 mm gravel exhibit the smallest difference between column-averaged and local moisture characteristics (Figure 7). Although the gravity corrections should yield some improvements in this 2 mm gravel when tested in a 30 mm tall column, the calculated 30 mm moving average fit does not track through many of the original data points. For this grain size, use of a taller column would have clearly necessitated gravity corrections, while use of a shorter column may not require corrections.

5. Concluding Comments

[12] Drainage moisture characteristic curves were obtained on well-sorted fractions of Hanford gravel. For this purpose, a method for accounting for hydrostatic saturation profiles within columns was developed and tested. For the 30 mm tall columns used in these tests, gravity corrections were clearly necessary in the 9 and 5 mm grain size gravels. Integration of curve-fits to the corrected S(h) relations in these cases closely matched the original column-averaged drainage curves. Results from experiments with 2.0–2.4 mm gravel showed marginal need for the gravity correction when 30 mm tall columns are used.

[13] Two other factors besides mean grain size and column height also influence whether or not gravity corrections are needed in measurements of moisture characteristics in water-air systems. These are the grain size distribution and water-air surface tension. For a given average grain size, more monodisperse systems will require gravity corrections because the matric head interval associated with drainage (as well as rewetting) reduces to a very narrow range. Conversely more polydisperse systems will require less gravity correction since they include finer pores that generally diminish the moisture capacity in the region of maximum capacitance. Lowering surface tension will lead to requiring gravity corrections in finer grain size systems, in a manner predictable from Miller-Miller scaling [*Miller and Miller*, 1956; *Elrick et al.*, 1959].

References

Brooks, R. H., and A. T. Corey, Hydraulic properties of porous media, *Hydrol. Pap. 3*, Colo. State Univ., Fort Collins, 1964.

Buckingham, E. A., Studies of the movement of soil moisture, *U.S. Dep. Agric. Bur. Soils Bull.*, *38*, 61 pp., 1907.

Conca, J. L., M. J. Apted, W. Zhou, R. C. Arthur, and J. H. Kessler, Flow barrier system for long-term high-level-waste isolation: Experimental results, *Nucl. Technol.*, *124*, 88–99, 1998.

Dane, J. H., M. Oostrom, and B. C. Missildine, An improved method for determination of capillary pressure-saturation curves involving TCE, water, and air, *J. Contam. Hydrol.*, *11*, 69–81, 1992.

Elrick, D. E., J. H. Scandrett, and E. E. Miller, Testing of capillary flow scaling, *Soil Sci. Soc. Am. Proc.*, *23*, 329–332, 1959.

Haines, W. B., Studies in the physical properties of soil, V, The hysteresis effect in capillary properties, and the modes of moisture distribution associated therewith, *J. Agric. Sci.*, *20*, 97–116, 1930.

Jalbert, M., and J. H. Dane, Correcting laboratory retention curves for hydrostatic fluid distributions, *Soil Sci. Soc. Am. J.*, *65*, 648–654, 2001.

Klute, A., Water retention: Laboratory methods, in *Methods of Soil Analysis*, part 1, *Physical and Mineralogical Methods, Agron. Monogr.*, vol. 9, 2nd ed., pp. 635–662, Am. Soc. Agron., Madison, Wis., 1986.

Krumbein, W. C., and L. L. Sloss, *Stratigraphy and Sedimentation*, 2nd ed., W. H. Freeman, New York, 1963.

Leverett, M. C., Capillary behavior in porous solids, *Trans. Am. Inst. Mining Metall. Eng.*, *142*, 152–169, 1941.

Liu, H. H., and J. H. Dane, Improved computational procedure for retention relations of immiscible fluids using pressure cells, *Soil Sci. Soc. Am. J.*, *59*, 1520–1524, 1995.

Luthin, J. N., and P. R. Day, Lateral flow above a sloping water table, *Soil Sci. Soc. Am. Proc.*, *19*, 406–410, 1955.

Miller, E. E., and R. D. Miller, Physical theory for capillary flow phenomena, *J. Appl. Phys.*, *4*, 324–332, 1956.

Rhoades, K., B. N. Bjornstad, R. E. Lewis, S. S. Teel, K. J. Cantrell, R. J. Serne, J. L. Smoot, C. T. Kincaid, and S. K. Wurstner, Estimation of the release and migration of lead through soils and groundwater at the Hanford Site 218-E-12B burial ground, vol. 2, Appendices, *PNL-8356 Vol. 2, UC-603*, Pac. Northwest Lab., Richland, Wash., 1992.

Schroth, M. H., S. J. Ahearn, J. S. Selker, and J. D. Istok, Characterization of Miller-similar silica sands for laboratory hydrologic studies, *Soil Sci. Soc. Am. J.*, *60*, 1331–1339, 1996.

van Genuchten, M. T., A closed-form equation for predicting the hydraulic conductivity of unsaturated soils, *Soil Sci. Soc. Am. J.*, *44*, 892–898, 1980.

K. R. Olson, T. K. Tokunaga, and J. Wan, Earth Sciences Division, Lawrence Berkeley National Laboratory, Berkeley, CA 94720, USA. (tktokunaga@lbl.gov)